Inorganic Chemistry

Article

pubs.acs.org/IC

Complexation of Europium(III) by Bis(dialkyltriazinyl)bipyridines in 1-Octanol

Michael Steppert,*[,†] Ivana Císařová,[‡] Thomas Fanghänel,[§,⊥] Andreas Geist,[†] Patric Lindqvist-Reis,[†] Petra Panak,[†,⊥] Petr Štěpnička,[‡] Sascha Trumm,[†,⊥] and Clemens Walther[†]

[†]Institute for Nuclear Waste Disposal, Karlsruhe Institute of Technology, P.O. Box 3640, 76021 Karlsruhe, Germany

[‡]Department of Inorganic Chemistry, Faculty of Science, Charles University in Prague, Hlavova 2030, 128 40 Praha 2, Czech Republic

[§]Institute for Transuranium Elements, European Commission, Joint Research Centre, 76125 Karlsruhe, Germany

[⊥]Physikalisch-Chemisches Institut, Ruprecht-Karls Universität Heidelberg, 69047 Heidelberg, Germany

Supporting Information

ABSTRACT: The present work focuses on highly selective ligands for An^{III}/Ln^{III} separation: bis(triazinyl)bipyridines (BTBPs). By combining time-resolved laser-induced fluorescence spectroscopy, nanoelectrospray ionization mass spectrometry, vibronic sideband spectroscopy, and X-ray diffraction, we obtain a detailed picture of the structure and stoichiometry of the first coordination sphere of Eu^{III}-BTBP complexes in an octanolic solution. The main focus is on the 1:2 complexes because extraction studies revealed that those are the species extracted into the organic phase. The investigations on europium(III) complexes of BTBP with different triazin alkylation revealed differences in the formed complexes due to the bulkiness of the ligands. Because of the vibronic sidebands in the fluorescence spectra, we were able to detect whether or not nitrate ligands are coordinated in the first coordination sphere of the Eu-BTBP complexes. In solution, less sterically demanding BTBP offers enough space for additional coordination of anions and/or solvent molecules to form 9-coordinated Eu-BTBP 1:2 complexes, while bulkier ligands tend to form 8-fold-coordinated structures. We also report the first crystal structure of a Ln-BTBP 1:2 complex and that of its 1:1 complex, both of which are 10-coordinated.

1. INTRODUCTION

Separating trivalent actinides (An^{III}) from lanthanides (Ln^{III}) is a key issue within the "partitioning and transmutation" (P&T) strategy.[1] The concept is to separate actinides from spent nuclear fuel and recycle them in nuclear reactors rather than dispose of them in a final repository. Possible advantages would be a significantly reduced long-term radiotoxicity and heat load of the highly radioactive wastes to be disposed of in a deep geologic repository.

The actinide elements contained in spent nuclear fuel (U, Np, Pu, Am, and Cm) must be separated from approximately 40 other elements (fission products and activation products). Both hydrometallurgical and pyrometallurgical separation processes are considered and studied.

One of the more developed separation schemes is an extension to the industrially operated PUREX process:

The spent nuclear fuel is dissolved in nitric acid; U, Pu, and (with slight modifications to the process) Np are separated in the PUREX process, using tri-*n*-butyl phosphate (TBP) as the extracting agent. Next, Am, Cm, and Ln are extracted from the PUREX raffinate using alkylated malonamides or diglycolamides as extracting agents. Finally, Am and Cm are separated from Ln. The last step is the most challenging one: The chemistry of the trivalent cations Am and Cm is very similar to that of trivalent Ln ions. Thus, Am^{III} and Cm^{III} cannot be separated from Ln^{III} with common extracting agents coordinating via oxygen-donor atoms. Soft donor atoms such as sulfur or nitrogen are required to achieve sufficient selectivity.

6,6′-Bis(5,6-dialkyl-1,2,4-triazin-3-yl)-2,2′-bipyridines (BTBPs) selectively extract Am^{III} and Cm^{III} from nitric acidic solutions with good selectivity over Ln^{III}.[2−10] 6,6′-Bis(5,5,8,8-tetramethyl-5,6,7,8-tetrahydrobenzo-1,2,4-triazin-3-yl)-2,2′-bipyridine ($CyMe_4$-BTBP; Figure 1, top) is the current European reference molecule for An^{III}/Ln^{III} separation process development.[8,11−15]

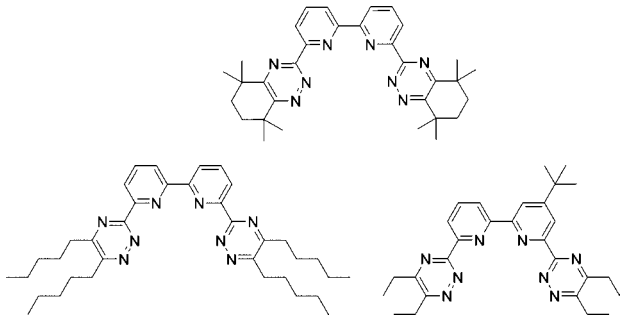

Figure 1. BTBP ligands used in this study: $CyMe_4$-, C5-, and *t*-Bu-C2-BTBP.

Several previous studies have investigated the complexation behavior of BTBP toward An^{III} and Ln^{III}. In extraction studies, it was shown that the $M(BTBP)_2(NO_3)_3$ species is extracted

Received: September 30, 2011
Published: December 1, 2011

   dx.doi.org/10.1021/ic202119x | *Inorg. Chem.* 2012, 51, 591−600

into the organic phase.[6,12,15] Single-crystal X-ray diffraction studies on different Ln^{III}-BTBP 1:1 complexes have shown that BTBP acts as a tetradentate chelating ligand coordinating via the two pyridine and two N^2 triazin nitrogen atoms. Two structurally different 10-coordinate $[Ln(C2\text{-}BTBP)(NO_3)_3]$ complexes were found for La−Er, while only 9-coordinate $[Ln(C2\text{-}BTBP)(NO_3)_2(H_2O)](NO_3)$ complexes were obtained for Yb−Lu.[16] However, by numerous solution studies, BTBP is known to extract An^{III} and Ln^{III} as 1:2 complexes;[15] e.g., for Gd^{III} 1:2 complexes, $CyMe_4$-BTBP and C1-BTBP (R = CH_3) were clearly identified by relaxivity titrations in acetonitrile.[17] Also in aqueous solution 1:2 complexes appear to be the dominating species, e.g., $[M(t\text{-}Bu\text{-}C2\text{-}BTBP)_2(H_2O)]^{3+}$ (M = Cm, Eu), as was recently identified by TRLFS.[18] A Eu^{III} complex of the same composition was also found in water-saturated 1-octanol.[19] On the other hand, an 8-coordinate $[Eu(BTBP)_2]^{3+}$ complex was postulated to be the dominating species in 1-octanol not previously saturated with water. In contrast, an electrospray ionization mass spectrometry (ESI-MS) study on Am^{III}- and Eu^{III}-BTBP complexes prepared by extraction into an organic phase consisting of BTBP in different diluents, among them 1-octanol (which thus is water-saturated), reported the exclusive formation of $[M(BTBP)_2(NO_3)_x]^{(3-x)+}$ (x = 0, 1) species. From those experiments, it was concluded that one nitrate ion (x = 1) was bonded to the metal ion.[12] Considering this relatively large body of data showing that the 1:2 complex is dominating in solution, it is somewhat surprising that no crystal structure of a 1:2 complex with BTBP has been reported up to now. In this study, we were able to obtain single crystals of the double salt $[Eu(CyMe_4\text{-}BTBP)_2(NO_3)][Eu(NO_3)_5]$ (**1**). However, recrystallization of **1** in dichlormethane/acetonitrile transformed it into the 1:1 complex $[Eu(CyMe_4\text{-}BTBP)(NO_3)_3]$ (**2**).

The present paper focuses on complexation between Eu^{III} and $CyMe_4$-BTBP, C5-BTBP, and *t*-Bu-C2-BTBP (Figure 1) in an octanol solution not saturated with water, and the main aim is to identify and characterize these complexes. Note that the *t*-Bu-C2-BTBP ligand sometimes is called MF1-BTBP in the literature. Of special interest is the location of the anion(s) perchlorate and nitrate in the complexes and to which extent different alkyl moieties on the BTBP ligands have an influence on this. Because extraction of the An^{III} ions takes place between the organic (1-octanol) phase and the nitric acid aqueous phase, which contains the An^{III}/Ln^{III} mixture, understanding the role of the nitrate ions is crucial for improving the ligand and the extraction process. Even if the perchlorate system is not process-relevant, it is studied here for the sake of comparison because it provides simpler coordination chemistry than the nitrate system. The more complex coordination chemistry of the latter system is due to the fact that nitrate ions tend to form inner-sphere complexes with lanthanide/actinide ions and thus compete with the BTBP ligands for coordination.

To characterize the different Eu^{III}-BTBP complexes in solution, we used time-resolved laser-induced fluorescence spectroscopy (TRLFS), vibronic sideband spectroscopy (VSBS), and nanoelectrospray-ionization time-of-flight mass spectrometry (nano-ESI-TOF-MS). TRLFS is known for its ability to probe the chemical environment of fluorescent ions such as Eu^{III} and Cm^{III} [19−23] and was recently used to study the complexation of Eu^{III} with BTP and BTBP.[18,19,24−27] Information about the complexes' coordination stoichiometry was obtained by measuring the fluorescence lifetime, from which we calculated the number of quenching molecules (octanol and water) in the first coordination sphere. By analysis of the splitting of the $^5D_0 \rightarrow {}^7F_{1,2}$ transitions, it was possible in some cases to obtain information about the local symmetry. In addition, the weak vibronic sidebands (VSBs) accompanying the electronic transitions provide information on whether or not the nitrate ions are coordinating to Eu^{III}. The electrospray ionization technique is a soft method to transfer ions from solutions to the gas phase.[28] It is broadly applied to investigate macromolecules[29−31] but is also a powerful method to analyze hydrolysis reactions of metal cations like Zr^{IV},[32] Th^{IV},[33] and Pu^{IV} [34] and was also applied to study extraction ligands.[12,24,35−37]

2. EXPERIMENTAL SECTION

2.1. Sample Preparation. *2.1.1. Solutions.* Stock solutions (10^{-2} mol/L) of C5-, *t*-Bu-C2, and $CyMe_4$-BTBP (ligands were received from the University of Reading, Reading, U.K.) were prepared by dissolving weighed amounts of the corresponding ligands in 1-octanol (Merck). The solutions were prepared freshly before use because the ligand is only stable for some days in solution. For the TRLFS measurements, titrations were performed by the addition of appropriate amounts of ligand stock solution to the 10^{-4} mol/L $Eu(ClO_4)_3$- and $Eu(NO_3)_3$/1-octanol solutions [obtained by dissolving $Eu(ClO_4)_3{\cdot}6H_2O$ and $Eu(NO_3)_3{\cdot}6H_2O$ (Alfa-Aesar) in 1-octanol]. With *t*-Bu-C2-BTBP and C5-BTBP, solutions were equilibrated for 20 min before the spectra were recorded, which was shown in preliminary studies to be sufficient to reach equilibration, while with $CyMe_4$-BTBP, 90 min was necessary to reach equilibrium. In one of the experiments, O-deuterated 1-octanol was used, obtained by H/D exchange by the addition of 99% D_2O to the solution, followed by evaporation of excess water by vigorous stirring in vacuo overnight, a procedure that was repeated twice. The two 1-octanol solutions used in the nano-ESI-TOF-MS studies both contain 1×10^{-4} mol/L $Eu(NO_3)_3$ but have different C5-BTBP concentrations, 2.5×10^{-5} and 1×10^{-4} mol/L, respectively. 1-Octanol was used as purchased from Merck. This means that it contains a significant fraction of water (about 20 mmol/L).

2.1.2. Solid Samples. A total of 26.5 mg (6.2×10^{-5} mol) of $CyMe_4$-BTBP was dissolved in dichloromethane (5 mL), and the solution was added to 21.5 mg of $Eu(NO_3)_3{\cdot}6H_2O$ (4.8×10^{-5} mol) dissolved in acetonitrile (5 mL). The resulting colorless solution was allowed to crystallize by slow evaporation at room temperature, yielding platelike colorless crystals having the composition $[Eu(CyMe_4\text{-}BTBP)_2(NO_3)][Eu(NO_3)_5]$ (**1**). A small part of this material was removed from the solution for single-crystal X-ray measurements, while the rest was dissolved in the mother liquor, which was thereafter left at room temperature to crystallize. As the solution volume was reduced, well-developed prism-shaped single crystals of $[Eu(CyMe_4\text{-}BTBP)(NO_3)_3]$ (**2**) were formed. Crystals of $[Eu(C2(BTBP))(NO_3)_3]{\cdot}MeCN$ (**3**) were synthesized following the procedure described in ref 16. Single crystals having the composition $[Eu(t\text{-}Bu\text{-}C2\text{-}BTBP)_2(CF_3SO_3)](CF_3SO_3)_2$ (**4**) were obtained after slow evaporation at room temperature of an ethanol solution of stoichiometric amounts of $Eu(CF_3SO_3)_3$ (Sigma-Aldrich) and *t*-Bu-C2-BTBP.

2.2. Crystallography. Selected crystals of **1** and **2** were mounted in glass capillaries (to avoid decomposition) and transferred to a Nonius Kappa CCD image-plate diffractometer. The diffraction data were collected at 150(2) K using monochromatized Mo Kα radiation (λ = 0.710 73 Å), and Gaussian absorption corrections based on the crystal shape were applied (μ = 1.68 mm^{-1}). The structure was solved by direct methods (*SIR2002*)[38] and refined by full-matrix least squares based on F^2 (*SHELXH*).[39] All non-hydrogen atoms but those involved in disordered moieties were refined anisotropically [Crystal data for **1**: $C_{68}H_{82}Eu_2N_{24}O_{18}$, orthorhombic, a = 27.42330(10) Å, b = 20.2058(2) Å, c = 28.1096(2) Å; space group *Pbca* (No. 61), Z = 8, V = 15575.8(2) $Å^3$, T = 150(2) K, 328 445 reflections measured, 13 334 reflections with $I > 2\sigma(I)$, 17 190 independent reflections (R_{int} = 0.11),

dx.doi.org/10.1021/ic202119x | *Inorg. Chem.* 2012, 51, 591−600

1005 parameters, 3 restraints, GOF = 1.07, final $R(F^2)$ = 0.044 [for 17 190 data with $I > 2\sigma(I)$], $wR(F^2)$ = 0.106 (all data), max/min residual electron density 2.56/−2.16 e/Å^3. Crystal data for **2**: $C_{32}H_{38}Eu_1N_{11}O_9$, triclinic, a = 11.23450(10) Å, b = 11.69120(10) Å, c = 16.1069 (2) Å, α = 90.6795(5)°, β = 101.1741(6)°, γ = 115.3993(6)°, space group $P\bar{1}$ (No. 2), V = 1864.04(3) Å^3, T = 150(2) K, 60 405 reflections measured, 8051 reflections with $I > 2\sigma(I)$, 8511 independent reflections (R_{int} = 0.033), 479 parameters, 9 restraints, GOF = 1.05, final $R(F^2)$ = 0.023 [for 17 190 data with $I > 2\sigma(I)$], $wR(F^2)$ = 0.057 (all data), max/min residual electron density 1.26/−1.13 e/Å^3], while hydrogen atoms bound to carbon atoms were added at idealized positions and refined using a riding model. Crystal data were also collected for **4** at 200 K on a Siemens SMART CCD 1000 diffractometer. However, although the crystal structure (solved in the monoclinic space group $P2_1/c$) unambiguously showed the compound to consist of $[Eu(C2\text{-}BTBP)_2(CF_3SO_3)]^{2+}$ and CF_3SO_3 entities, a satisfactory structure refinement failed because of severe disorder of the triflate anions, which probably is caused by a low crystal quality.

2.3. TRLFS. An XeCl excimer (Lambda Physics, EMG, 308 nm) pumped dye laser (Lambda Scanmate; pulse width 20 ns, spectral width 0.2 cm^{-1}) was used for excitation, with the excitation wavelength set to 394 nm using the laser dye QUI. For direct excitation to the Eu($^5D_0$) electronic level, Coumarin153 was used as the laser dye.[20] All emission spectra were recorded with an ANDOR iStar camera system, equipped with 400, 1200, and 2400 lines/mm gratings. To measure the decay time of the fluorescence emission, the intensifier was opened for 10 ms at variable delay periods after the laser excitation pulse in steps of 10−100 μs depending on the emission lifetime (τ), the latter of which was obtained by fitting the integrated intensity (I) at time t after the laser pulse to $I(\lambda) = I_0(\lambda)\exp(-t/\tau)$, where I_0 is the intensity at t = 0.

The solutions were contained in quartz cuvettes, while the solid sample (**3**) was mounted on an in-house-constructed copper sample holder, attached to the cold head of the cryostat (Cryodyne Cryocooler model 22C, compressor 8200, CTI-Cryogenics, USA) and measured at 20 K. The holographic 2400 lines/mm grating was used for high-resolution $^5D_0 \rightarrow {}^7F_0$ spectra. Because the $^7F_0$ and $^5D_0$ levels are nondegenerate, Eu^{III} species with different chemical/structural environments provide unique $^5D_0 \rightarrow {}^7F_0$ transitions. The $^7F_0$ position reflects the coordination strength exerted by the ligands: stronger interactions generally give rise to a slight bathochromic shift; for example, upon complexation with BTBP, the shift is ∼2 nm.[40−42] In addition, the splitting and relative intensity of the $^5D_0 \rightarrow F_1$ (magnetic dipole) and $^5D_0 \rightarrow F_2$ (electric dipole; hypersensitive) transitions give information about the local symmetry,[43] which together with the information obtained from the emission lifetime (τ) allow an approximate determination of the stoichiometry of the studied complex. Using the refined and extended equation $q = 1.11(\tau_{H_2O}{}^{-1} - \tau_{D_2O}{}^{-1} - 0.31 - 0.45n_{OH})$, we may calculate the number of quenchers q, water and octanol molecules, in the first coordination sphere of Eu^{III},[44] where the nonradiative energy transfer of an OH alcohol group is ∼45% that of a water molecule.[19,45,46] A systematic quantification of the numbers of water/alcohol quenchers to Eu^{III} as a function of the concentration of water in 1-octanol was recently performed.[19] In cases when several chemically/structurally unique Eu^{III} ions are present simultaneously in solution their respective lifetimes and emission spectra can be obtained using selective, direct excitation.[20]

2.4. VSBS. By VSBS, the types of coordinated ligands can be determined.[47,48] Those sidebands have their origin in the coupling of electronic transitions and the vibrational modes of the ligands (called vibronic coupling), leading to Stokes-shifted side peaks of the corresponding electronic transition.[48] Free NO_3^- (trigonal planar) has D_{3h} symmetry. If the nitrate is coordinated in a bidentate fashion, the symmetry is lowered (C_{2v} and lower). This leads to a splitting of the $\nu_4(E')$ vibration band (725 cm^{-1}) to $\nu_5(A)$ and $\nu_3(A)$ with 710 and 740 cm^{-1} for C_1 symmetry.[49] Those values may vary depending on the differences in the ligand field. The vibronic interactions in compounds containing europium nitrate were studied in refs 48−50. We use the VSBs correlated to the ν_5 and ν_3 vibration transitions of coordinated nitrate because they do not overlap with the electronic transitions in the fluorescence spectra. For the measurement setup, see section 2.3.

2.5. Nano-ESI-TOF-MS Setup. TOF-MS was performed by coupling a home-built ESI source to an ALBATROS ESI-TOF-MS spectrometer.[51−54] Spray capillaries with an inner tip diameter of 2 μm from Proxeon (Odense, Denmark) were filled with 10 μL of the sample solution, and a voltage of 2100 V was applied to the capillaries to generate the electrospray. A static nitrogen pressure of <0.5 bar was applied to the end of the capillary to achieve a constant electrospray. Sample flow rates were approximately 15 nL/min. A nitrogen flow rate of approximately 0.5 L/min of ambient temperature was used for the gas curtain. The voltage between the orifice and skimmer was kept at 42 V. The ions present in the solution were detected by a TOF-MS spectrometer. Mass resolutions of up to $m/\Delta m$ = 26 000 are possible. In the present work, the spectrometer was operated at m/Δ = 14 000, still allowing for resolution of the isobaric species but providing higher sensitivity. Because of the soft conditions, the analyzed molecules remain in small solvent shells during the measurement, making it a method of low invasiveness.

3. RESULTS AND DISCUSSION

3.1. Crystal Structures. The unit cell of **1** comprises eight 10-coordinate cation and anion entities (Z = 8), $[Eu(CyMe_4\text{-}BTBP)_2(NO_3)]^{2+}$ and $[Eu(NO_3)_5]^{2-}$, in which nitrate ions are bound to europium in a bidentate fashion (Figure 2).

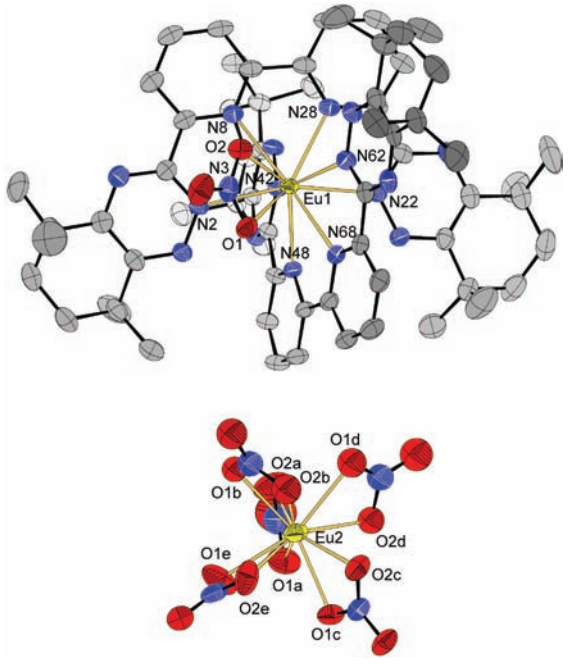

Figure 2. Crystal structures of the $[Eu(CyMe_4\text{-}BTBP)_2(NO_3)]^{2+}$ (top) and $[Eu(NO_3)_5]^{2-}$ (bottom) entities in **1** at 150 K. Displacement ellipsoids are drawn at the 50% probability level. Hydrogen atoms are omitted for clarity. Two nitrate anions are disordered in the $[Eu(NO_3)_5]^{2-}$ anion; for clarity, only the positions with larger occupational factors are displayed. Selected bond distances (in Å): Eu1−N48, 2.539(3); Eu1−O2, 2.540(3); Eu1−N62, 2.552(3); Eu1−N42, 2.556(3); Eu1−O1, 2.579(3); Eu1−N28, 2.582(3); Eu1−N2, 2.589(3); Eu1−N22, 2.589(3); Eu1−N8, 2.590(3); Eu1−N68, 2.599(3); Eu2−O2d, 2.432(4); Eu2−O2a, 2.440(5); Eu2−O1c, 2.444(3); Eu2−O1d, 2.465(5); Eu2−O2e, 2.473(4); Eu2−O1e, 2.480(4); Eu2−O2c, 2.486(3); Eu2−O1a, 2.491(4); Eu2−O1b, 2.531(6); Eu2−O2b, 2.582(6).

dx.doi.org/10.1021/ic202119x | Inorg. Chem. 2012, 51, 591−600

The anion in **1** is also found in several other compounds, e.g., $[(C_6H_5)_4As][Eu(NO_3)_5]$,[55] while the cation is the first reported structure of a 1:2 Ln-BTBP complex. Attempts to obtain the corresponding 8-coordinate 1:2 complex without the coordinating anion failed. With trifluoromethanesulfonate ($CF_3SO_3^-$), we obtained crystals comprising 9-coordinate cations in **4** (the two trifluoromethanesulfonate anions in the lattice are strongly disordered; the crystal data of this compound were therefore not included in this paper).

Complex **2** has near-C_2 symmetry, with three nitrate ions bidentately bound to the 10-fold-coordinated europium ion, which lies in the quasi-plane of the tetradentate chelating $CyMe_4$-BTBP ligand (Figure 3). The ligand deviates slightly from planar geometry, probably as a result of steric and/or packing effects. The Eu–N bond distances are narrowly distributed between 2.53 and 2.54 Å, while the Eu–O distances show a wider range, 2.46–2.60 Å. It is interesting to compare the structure of **2** with that of $[Eu(C2\text{-}BTBP)(NO_3)_3]$.[16] In the latter compound, the symmetry around the metal center is higher (C_2), the Eu–N distances are longer (~2.60 Å), and the Eu–O distances are more narrowly distributed (2.49–2.54 Å) than those in **2**.

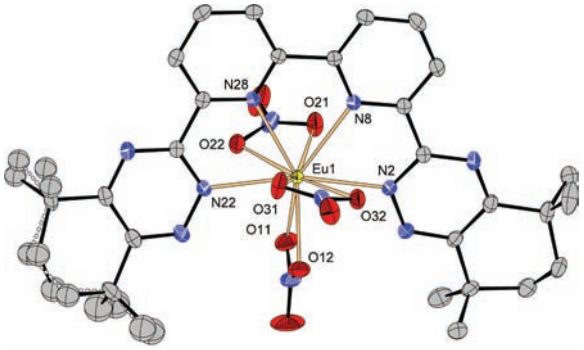

Figure 3. Crystal structure of **2** at 150 K. Displacement ellipsoids are drawn at the 50% probability level. Hydrogen atoms are omitted for clarity. The disordered atoms of the $CyMe_4$ group (left) are refined isotropically. Selected bond distances (in Å): Eu1–O12, 2.4597(17); Eu1–O11, 2.4642(17); Eu1–O31, 2.4752(18); Eu1–O21, 2.5071(17); Eu1–O22, 2.5282(16); Eu1–N28, 2.5333(18); Eu1–N8, 2.5340(17); Eu1–N2, 2.5401(18); Eu1–N22, 2.5442(18); Eu1–O32, 2.5998(17).

3.2. TRLFS. This section starts with the study of europium(III) perchlorate/1-octanol solutions at different concentrations of added $CyMe_4$-BTBP, C5-BTBP, and *t*-Bu-C2-BTBP, which is followed by the study of the corresponding europium(III) nitrate system. In contrast to the latter, the emission bands in the former system are sharp and their splitting (and thus the coordination symmetry) may be determined rather unambiguously.

3.2.1. Perchlorate System: The Octanol-Solvated Eu^{3+} Ion. The $^5D_0 \rightarrow {}^7F_0$ transition of the solvated Eu^{3+} ion in 1.0×10^{-4} mol/L $Eu(ClO_4)_3$/1-octanol solution appears as a fairly symmetric band at 579.0 nm (Figure 4). The emission decay is monoexponential with an emission lifetime of 180 μs, in good agreement with a recent TRLFS study of $Eu(ClO_4)_3$ in 1-octanol.[19] By assuming that perchlorate ions do not form inner-sphere complexes with Eu^{3+}, the obtained lifetime (180 μs) was found to be consistent with a mixed octanol/water complex with a stoichiometry of $[Eu(C_8H_{17}OH)_7(H_2O)]^{3+}$. Here the water fraction in 1-octanol was calculated

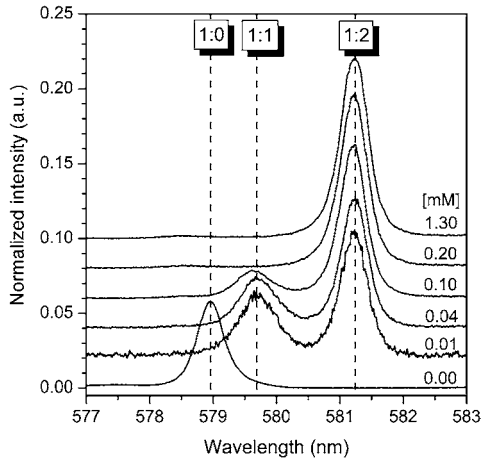

Figure 4. Emission spectra of the $^5D_0 \rightarrow {}^7F_0$ transition of a 1.0×10^{-4} mol/L $Eu(ClO_4)_3$/1-octanol solution upon the addition of $CyMe_4$-BTBP between 0.0 and 1.3×10^{-3} mol/L. The positions of the 1:0, 1:1, and 1:2 complexes are indicated.

as shown in the studies of Vu in ref 19. The notably longer lifetime of this complex compared to that of the Eu^{3+} aqua ion, ~110 μs, is due to the fact that the nonradiative energy transfer from the $^5D_0$ state to the OH vibrational overtones of octanol is less efficient than the energy transfer to the OH vibrational overtones of water.[19]

$CyMe_4$-BTBP. The addition of the $CyMe_4$-BTBP ligand from substoichiometric levels to a large excess (1.0×10^{-5}–1.3×10^{-3} mol/L) to the 1.0×10^{-4} mol/L $Eu(ClO_4)_3$/1-octanolic solution gives rise to two new bands with peak maxima at 579.6 and 581.2 nm, whose relative intensities depend on the ligand concentration (Figure 4). The low- and high-wavelength bands are assigned to the $[Eu(CyMe_4\text{-}BTBP)]^{3+}$ and $[Eu(CyMe_4\text{-}BTBP)_2]^{3+}$ complexes, respectively. From the marked difference of their intensities, it is obvious that most of the complexed Eu^{3+} ions are bound to two $CyMe_4$-BTBP molecules in a 1:2 complex, even at ligand concentrations of as low as 1.0×10^{-4} mol/L (1 equiv), while the 1:1 complex is strongly suppressed. However, because the fluorescence intensity factors, related to the quantum yield, of the complexed and noncomplexed ions are not known, it is uncertain to determine quantitatively the species distribution from the peak intensity, even though the fluorescence intensity factors most likely increase with increasing ligand complexation.

The determined emission lifetimes of the 1:1 and 1:2 complexes, 340 and 2000 μs, respectively, are used to determine the number of coordinating solvent molecules, octanol and water. According to a recent TRLFS study of $Eu(ClO_4)_3$ in octanol solution,[19] a lifetime of 340 μs corresponds to a coordination of one to two octanol molecules and one water molecule and 2000 μs to zero octanol molecules, suggesting the stoichiometries of the 1:1 and 1:2 complexes to be $[Eu(CyMe_4\text{-}BTBP)(C_8H_{15}OH)_{1-2}(H_2O)]^{3+}$ and $[Eu(CyMe_4\text{-}BTBP)_2]^{3+}$, respectively. Considering the fairly short lifetime (340 μs) of the 1:1 complex and that perchlorate ions are known to be weakly coordinating, it seems unlikely that they compete with solvent molecules for coordination.

C5-BTBP and t-Bu-C2-BTBP. Titration with C5-BTBP and *t*-Bu-C2-BTBP gives rise to the same $^5D_0 \rightarrow {}^7F_0$ spectra, with the same peak positions and peak shapes for the 1:1 and 1:2 complexes as those with $CyMe_4$-BTBP (see Figure S1 in the Supporting Information). This striking similarity is rational

dx.doi.org/10.1021/ic202119x | *Inorg. Chem.* 2012, 51, 591–600

because the difference between the ligands is small and refers only to the length and bulkiness of the alkyl side chain on the triazin part of the ligand, which have little influence on the electron density at the nitrogen-donor atoms. On the other hand, the structure of the alkyl side chain appears to be the main reason for the slower kinetics of the formation of the 1:2 complex with the bulkier $CyMe_4$-BTBP than with C5-BTBP and *t*-Bu-C2-BTBP (see section 2.1.1).

While the emission lifetimes of the 1:1 complexes of the three ligands are identical, 340 μs, the lifetimes of the respective 1:2 complexes are rather different, about 2000, 1400, and 1020 μs for $CyMe_4$-BTBP, C5-BTBP, and *t*-Bu-C2-BTBP, respectively. To check whether these differences are due to different nonradiative decay times of the ligands or different quenching contributions from nearby solvent molecules, we recorded time-resolved fluorescence spectra of the 1:2 complex of *t*-Bu-C2-BTBP in O-deuterated 1-octanol (saturated with D_2O) because OD vibrations do not quench the fluorescence.[45,46] Upon deuteration, the lifetime increased from about 1020 to 2000 μs, suggesting that this was due to coordination of a solvent molecule with exchangeable protons/deuterons. A coordination of one octanol molecule is in accordance with the number calculated using the equation by Supkowski et al., $n_{OH} \approx 1.2$ (1020 μs), while the corresponding numbers for $CyMe_4$-BTBP and C5-BTBP are $n_{OH} \approx 0.0$ (2000 μs) and 0.5 (1400 μs), respectively (see Table 1).

Table 1. Fluorescence Emission Lifetimes (in μs) and the Positions of the $^5D_0 \rightarrow {}^7F_0$ Transitions (within Parentheses in nm) of Identified Eu^{III} Complexes in a 1.0×10^{-4} mol/L $Eu(ClO_4)_3$/1-Octanol Solution upon Titration with Different BTBP Ligands (L)[a]

ligand (L)	1:0 complex	1:1 complex	1:2 complex
$CyMe_4$-BTBP	180 (579.0)	340 (579.6)	2000 (581.2)
C5-BTBP	180 (579.0)	340 (579.6)	1400 (581.2)
t-Bu-C2-BTBP	180 (579.0)		1020 (581.2)

[a]The stoichiometries of the 1:0, 1:1, and 1:2 complexes are $[Eu(C_8H_{17}OH)_7(H_2O)]^{3+}$, $[Eu(L)(C_8H_{17}OH)_{1-2}(H_2O)]^{3+}$, and $[Eu(L)_2(C_8H_{17}OH)_{0-1}]^{3+}$, respectively; see the text.

The different lifetimes of the respective 1:2 complexes are most likely due to steric effects because the electronic structures of the different ligands should not differ significantly from each other. The bulkier $CyMe_4$-BTBP ligand does not allow octanol molecules to come close enough to Eu^{III} to affect its emission lifetime, whereas with the sterically less demanding C5-BTBP and *t*-Bu-C2-BTBP ligands, the lifetimes are shorter as the probability for solvent molecules to approach the metal center is larger. This view is in agreement with the results from NMR relaxivity studies of $Gd(ClO_4)_3$ in acetonitrile with different BTBP ligands.[17] An alternative view would be an equilibrium between 8- and 9-coordinate complexes, for example, $[Eu(t\text{-Bu-C2-BTBP})_2(C_8H_{17}OH)]^{3+} \rightleftharpoons [Eu(t\text{-Bu-C2-BTBP})_2]^{3+} + C_8H_{17}OH$, which through fast solvent exchange would give an apparent coordination of less than one octanol molecule. In this model, the 1:2 complexes of the different BTBP ligands are expected to have slightly different spectra because the local symmetry is different for the 8- and 9-coordinated complexes. However, these 1:2 complexes have almost identical $^5D_0 \rightarrow {}^7F_0$ spectra (see Figure 5). The corresponding $^5D_0 \rightarrow {}^7F_{1-2}$ spectra are similar, but not identical,

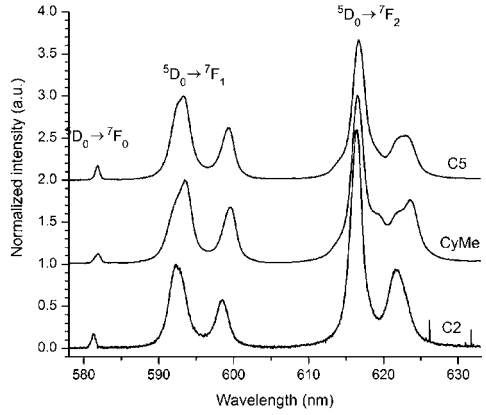

Figure 5. Emission spectra of the $^5D_0 \rightarrow {}^7F_{0-2}$ transitions of the 1:2 complexes of C5-, $CyMe_4$-, and *t*-Bu-C2-BTBP in a 1.0×10^{-4} mol/L $Eu(ClO_4)_3$/1-octanol solution with 1.3×10^{-3} mol/L BTBP.

showing 3- and 4-fold splitting, respectively (Figure 5). Quantum-chemical calculations on the $[Eu(CyMe_4\text{-BTBP})_2]^{3+}$ complex in the gas phase show tetragonal symmetry (square-antiprismatic coordination) with D_{2d} or S_4 point groups, leading to 2- and 3-fold splitting of the $^5D_0 \rightarrow {}^7F_1$ and $^5D_0 \rightarrow {}^7F_2$ transitions, respectively.[56] The splitting of these transitions indicates a slight deviation from this higher symmetry, most likely caused by the interaction or coordination of solvent molecules.

3.2.2. Nitrate System. Figure 6 shows selected $^5D_0 \rightarrow {}^7F_{0-2}$ spectra of the 1.0×10^{-4} mol/L $Eu(NO_3)_3$/1-octanol solutions

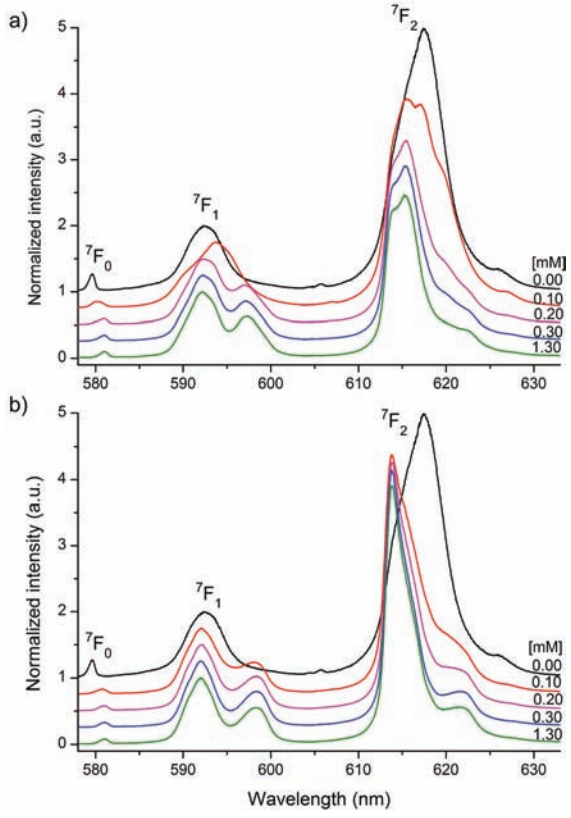

Figure 6. Emission spectra of the $^5D_0 \rightarrow {}^7F_{0-2}$ transitions of a 1.0×10^{-4} mol/L $Eu(NO_3)_3$/1-octanol solution upon the addition of (a) $CyMe_4$-BTBP and (b) *t*-Bu-C2-BTBP between 0.0 and 1.3×10^{-3} mol/L.

dx.doi.org/10.1021/ic202119x | *Inorg. Chem.* 2012, 51, 591–600

at different concentrations (1.0×10^{-5}–1.3×10^{-3} mol/L; 0–13 equiv) of added $CyMe_4$-BTBP and *t*-Bu-C2-BTBP (the corresponding spectra of C5-BTBP are very similar to those of *t*-Bu-C2-BTBP). Upon the addition of BTBP, the $^5D_0 \rightarrow {}^7F_0$ transition shifts to higher wavelengths, $^5D_0 \rightarrow {}^7F_1$ splits up, and the $^5D_0 \rightarrow {}^7F_2$ transition shifts to lower wavelengths. Although these spectroscopic changes express relatively large changes in the coordination, the splitting of the $^5D_0 \rightarrow {}^7F_{1,2}$ transitions is not clear-cut, which is likely due to a superposition of several spectra of complexes having different coordination structures. In order to obtain a more detailed picture about these complexes, high-resolution spectra of the $^5D_0 \rightarrow {}^7F_0$ transitions were recorded.

C5-BTBP. Figure 7a shows the high-resolution $^5D_0 \rightarrow {}^7F_0$ emission spectra of the 1.0×10^{-4} mol/L $Eu(NO_3)_3$ octanolic

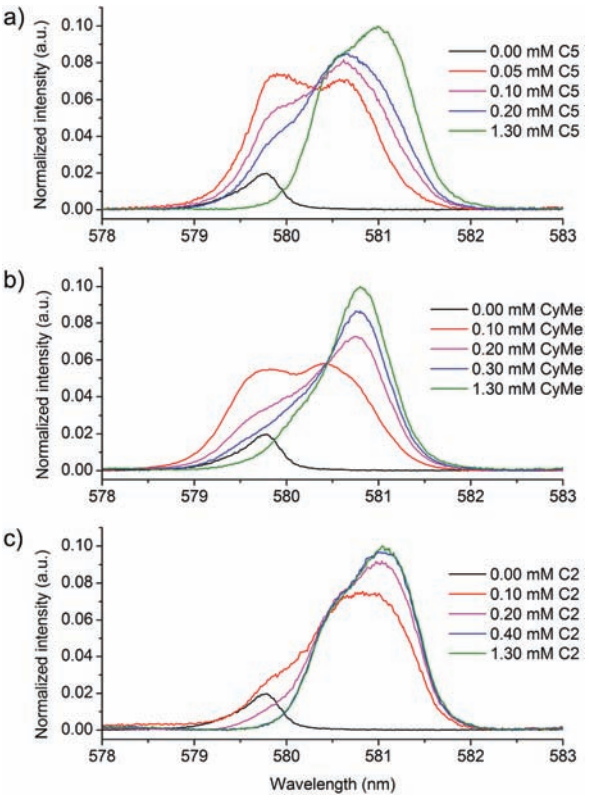

Figure 7. Emission spectra of the $^5D_0 \rightarrow {}^7F_0$ transition of a 1.0×10^{-4} mol/L $Eu(NO_3)_3$/1-octanol solution upon the addition of (a) C5-BTBP, (b) $CyMe_4$-BTBP, and (c) *t*-Bu-C2-BTBP between 0.0 and 1.3×10^{-3} mol/L.

solutions upon titration with C5-BTBP. With no ligand added, the solvated $Eu(NO)_3$ complex shows one emission band at 579.8 nm. The emission decay is monoexponential with an emission lifetime of ~430 μs, corresponding to a coordination of two octanol molecules and less than one water molecule; most likely, three to four bidentately bound nitrate ions complete the coordination shell (see the VSBS section below).[19]

The addition of a substoichiometric amount of C5-BTBP gives rise to two new bands at 579.9 and 580.6 nm (peak deconvolution of the spectra was used to obtain the band positions and intensities). The emission decay is no longer monoexponential, hinting at the presence of at least two Eu^{III} species with different emission lifetimes. Increasing the ligand concentration to 2×10^{-4} mol/L shifts the spectrum to the red because the intensity of the high-wavelength band increases at the expense of that at lower wavelength; the emission decay is biexponential with $\tau_1 \sim 1200$ and $\tau_2 \sim 2000$ μs, corresponding to $n_{OH} \approx 0.8$ and 0.0, respectively. On the basis of these lifetimes, we assign the band at 579.9 nm to the 1:1 complex with a possible stoichiometry of $[Eu(C5\text{-}BTBP)(NO_3)_x(C_8H_{17}OH)_{0-1}]^{3-x}$ ($x = 1$–2) and the band at 580.6 nm to the 1:2 complex $[Eu(C5\text{-}BTBP)_2(NO_3)_y]^{3-y}$ ($y = 0$–1). A further increase of the ligand concentration to 1.3×10^{-3} mol/L produces a slight additional red shift of the band, and the emission decay is nearly monoexponential with $\tau_1 \sim 2000$ μs, indicating one major Eu^{III} solution complex with $n_{OH} \approx 0.0$; see Table 2.

Table 2. Fluorescence Emission Lifetimes (in μs) and the Positions of the $^5D_0 \rightarrow {}^7F_0$ Transitions (within Parentheses in nm) of Identified Eu^{III} Complexes in a 1.0×10^{-4} mol/L $Eu(NO_3)_3$/1-Octanol Solution upon Titration with Different BTBP Ligands (L)[a]

ligand (L)	1:0 complex	1:1 complex	1:2 complex
$CyMe_4$-BTBP	430 (579.8)	1200 (580.4)	2000 (580.8)
C5-BTBP	430 (579.8)	900, 1200 (579.9, 580.6)	2000 (581.0)
t-Bu-C2-BTBP	430 (579.8)	1700 (580.6)	2000 (581.0)

[a]The stoichiometries of the 1:0, 1:1, and 1:2 complexes are $[Eu(NO_3)_x(C_8H_{17}OH)_y(H_2O)_z]^{3+}$, $[Eu(L)(NO_3)_x(C_8H_{17}OH)_{0-1}]^{(3-x)+}$ ($x = 1$–2), and $[Eu(L)_2(NO_3)_y]^{(3-y)+}$ ($y = 0$–1), respectively; see the text.

Because more than two different Eu^{III} species are expected to be present in solution at low ligand concentrations, fitting the emission decay profile to a biexponential function is not adequate. With 0.5 equiv of C5-BTBP, the concentration of noncomplexed $Eu(NO_3)_3$ species is not negligible. The emission lifetime of this species (~430 μs) may therefore be fixed in the fitting routine in order to determine the lifetimes of the remaining species. Because the lifetime value of ~2000 μs, obtained for the solutions with higher ligand concentrations, does not fit the emission decay profiles of the solutions with intermediate ligand concentrations, the more appropriate value of 1200 μs was then fixed as an upper limit. While these two lifetimes are still not sufficient to describe the multiexponential decays satisfactorily, a third lifetime corresponding to a third species in solution is needed. This latter value was estimated to be about 900 μs from the time-resolved measurement of the VSB spectra (see below). Thus, a triexponential decay with lifetimes fixed at 430, 900, and 1200 μs fits the data with high precision. This procedure was also used to account for the emission lifetimes of the different species in the solution with 1 equiv of C5-BTBP. In this case, the triexponential fit with lifetimes values of 900, 1200, and 2000 μs perfectly describes the emission decay, in line with the expectation that the amount of noncomplexed $Eu(NO_3)_3$ species is insignificant in solution at higher ligand concentrations.

$CyMe_4$-BTBP and t-Bu-C2-BTBP. The evolution of the $^5D_0 \rightarrow {}^7F_0$ spectra with increasing $CyMe_4$-BTBP concentration is similar to that of C5-BTBP (cf. Figure 7a,b). At low ligand concentrations, three different complexes are present in solution simultaneously: $[Eu(NO_3)_3(C_8H_{17}OH)_2(H_2O)]$ (τ = 430 μs; note that the stoichiometry of this complex is based on the fluorescence lifetime study in ref 19), $[Eu(CyMe_4\text{-}BTBP)(NO_3)_x(C_8H_{17}OH)_{0-1}]^{(3-x)+}$ ($x = 1$–2; τ = 1200 μs), and

dx.doi.org/10.1021/ic202119x | *Inorg. Chem.* 2012, 51, 591–600

$[Eu(CyMe_4\text{-}BTBP)_2(NO_3)_y]^{(3-y)+}$ (y = 0−1; τ = 2000 μs), while at higher ligand concentrations, only the 1:2 complex remains. The spectra evolution upon titration with *t*-Bu-C2-BTBP differs slightly from that with the other ligands; however, the 1:0 (430 μs), 1:1 (1700 μs), and 1:2 (2000 μs) complexes are detected (Figure 7c).

Table 2 summarizes the spectroscopic results obtained in the nitrate system.

3.3. VSBS. The $^5D_0 \rightarrow {}^7F_0$ emission spectrum of [Eu(C2-BTBP)$(NO_3)_3$]·MeCN (**3**) at 20 K shows a narrow band with a peak maximum at 580.87 nm (Figure 8a). The shoulder at the

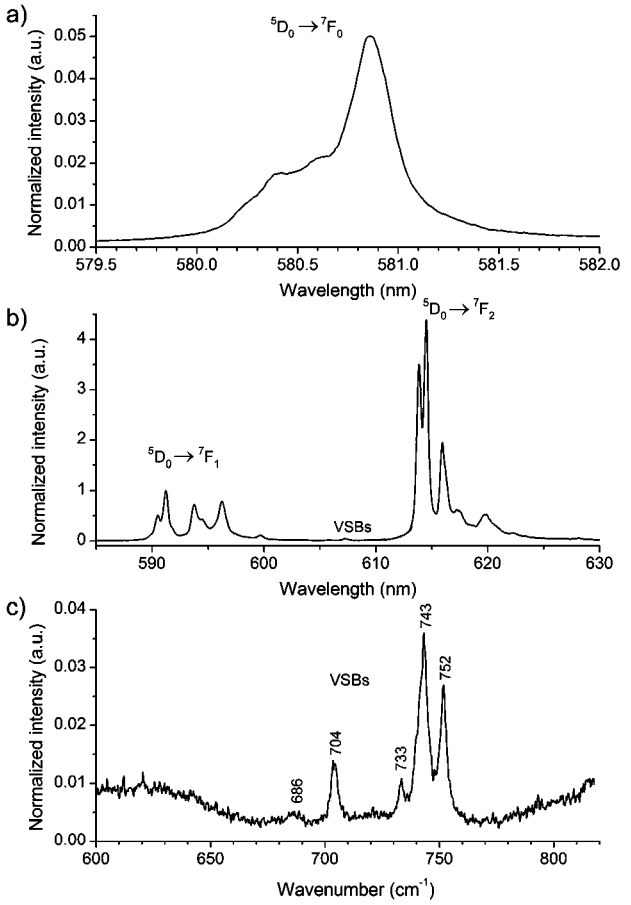

Figure 8. (a) $^5D_0 \rightarrow {}^7F_0$ emission spectrum (λ_{ex} = 394.0 nm) of [Eu(*t*-Bu-C2-BTBP)$(NO_3)_3$]·MeCN (**3**). The emission band with λ_{max} = 580.87 nm is assigned to that of **3**, while the shoulders at the low-wavelength side of the band are most likely due to nonreacted europium from the mother liquid (see the text). (b) $^5D_0 \rightarrow {}^7F_{1-2}$ emission spectrum upon direct excitation (λ_{ex} = 580.87 nm). Note the weak VSBs appearing between the $^5D_0 \rightarrow {}^7F_1$ and $^5D_0 \rightarrow {}^7F_2$ bands. (c) VSB spectrum of **3**. The ZPL is at 580.87 nm. $T \sim 20$ K.

bands' low-wavelength side is likely due to a residue from the mother liquid containing europium nitrate. To selectively excite Eu^{3+} in **3**, the wavelength was set to 580.87 nm. Figure 8b shows the emission spectrum of the corresponding $^5D_0 \rightarrow {}^7F_1$ and $^5D_0 \rightarrow {}^7F_2$ transitions. The weak features appearing in the region between these transitions are recognized as VSBs, originating from the transitions from the $^5D_0$ state to various vibrational levels of bound nitrate ions. The wavenumber differences between these bands, centered at 605.6, 606.7, 607.1, and 607.4 nm (the accuracy is ca. ±0.02 nm), and the zero-phonon line (ZPL) at 580.87 nm are 704, 733, 743, and 752 cm^{-1}, respectively, and are in accordance with values published for VSBs of $EuNO_3$ entities in various compounds (Figure 8c);[48−50] e.g., in the Raman and VSB spectra of $[Eu(NO_3)_3(bpy)_2]$·bpy, the in-plane deformation modes of bidentately bound nitrate ions were found at 706 (ν_5) and 735−742 (ν_3) cm^{-1}, respectively.[50] Therefore, we assign the band at 704 cm^{-1} to ν_5 and the bands at 733, 743, and 752 cm^{-1} to ν_3. The rather wide spread of the ν_3 vibrations may be understood by the likewise wide spread of the N−O bond distances of the bidentately coordinated nitrate ions.[16]

We now look at the solution spectra to see if they too reveal VSBs of bound nitrate ions. In the high-resolution emission spectrum of the $Eu(NO_3)_3$/octanol solution in Figure 9a, the

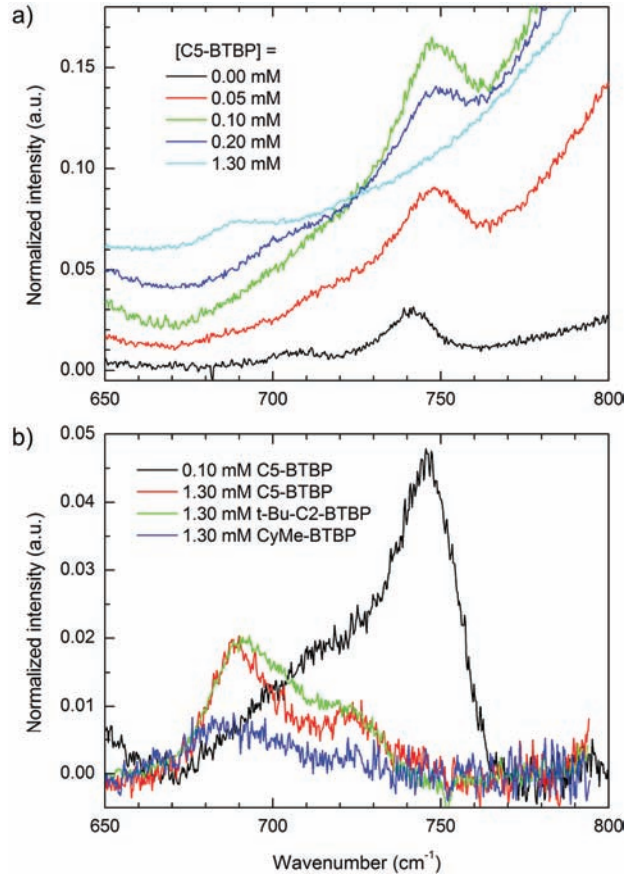

Figure 9. (a) VSB spectra of the "nitrate region" of a 1.0 × 10^{-4} mol/L $Eu(NO_3)_3$/1-octanol solution at different concentrations of added C5-BTBP between 0.0 and 1.3 × 10^{-3} mol/L. (b) Comparison of baseline-corrected VSB spectra of a 1.0 × 10^{-4} mol/L $Eu(NO_3)_3$/1-octanol solution at 0.1 and 1.3 × 10^{-3} mol/L C5-BTBP and 1.3 × 10^{-3} mol/L *t*-Bu-C2-BTBP and $CyMe_4$-BTBP. The ZPL corresponds to the $^5D_0 \rightarrow {}^7F_0$ band.

two weak bands at 604.3 (700 cm^{-1}; ν_5) and 605.5 nm (743 cm^{-1}; ν_3) are consistent with in-plane deformation modes of nitrate ions in $[Eu(NO_3)_3(C_8H_{17}OH)_2(H_2O)]$. By the addition of C5-BTBP, these bands disappear and two new similar but red-shifted bands appear at 605.2 (701 cm^{-1}; ν_5) and 607.0 (748 cm^{-1}; ν_3) nm. The positions of the latter are in accordance with those in **3**, confirming that they belong to the 1:1 complex $[Eu(NO_3)_3$(C5-BTBP)] (note that the emission intensity of this complex is much higher than that of the noncomplexed, solvated ion in 1-octanol). Moreover, the emission lifetime of the 748 cm^{-1} band is measured to be

dx.doi.org/10.1021/ic202119x | *Inorg. Chem.* 2012, 51, 591−600

~900 μs for the C5-BTBP system (this lifetime was used in the triexponential fit in section 3.2.2). At ligand concentrations above ~1.0×10^{-4} mol/L, the intensities of the ν_5 and ν_3 bands decrease. This is shown for C5-BTBP in Figure 9b, but the picture is very similar for *t*-Bu-C2-BTBP and $CyMe_4$-BTBP. However, the VSB spectra of the corresponding 1:2 complexes are not all identical (Figure 9b). In addition to a broad band at 685 cm^{-1} assigned to ligand vibrational modes, a weaker band appears at 720 cm^{-1} for *t*-C2-BTBP and C5-BTBP but not for $CyMe_4$-BTBP. Again, steric effects are the most obvious reason for these differences. In the 1:2 complexes of the sterically less demanding *t*-C2-BTBP and C5-BTBP ligands, there is enough space for one nitrate ion, whereas for the bulkier $CyMe_4$-BTBP, the probability for a nitrate ion to enter the first coordination shell seems significantly smaller. In contrast to the bidentately bound nitrate ions in **1**–**3**, the VSB spectra of the solution complexes of $[Eu(NO_3)(C5\text{-}BTBP)_2]^{2+}$ and $[Eu(NO_3)(t\text{-}Bu\text{-}C2\text{-}BTBP)_2]^{2+}$ indicate monodentate coordination. The rational for this is that the ν_3 (748 cm^{-1}) band does not appear in the spectrum at high *t*-Bu-C2-BTBP and C5-BTBP concentrations, while the band at 720 cm^{-1} is clearly visible, which indicates a change in the symmetry of NO_3^- from C_{2v} to D_{3h} because of a weakening of the bond to Eu^{III} in the $[Eu(NO_3)(C5\text{-}BTBP)_2]^{2+}$ and $[Eu(NO_3)(t\text{-}Bu\text{-}C2\text{-}BTBP)_2]^{2+}$ complexes. The ν_5 and ν_3 modes of C_{2v} symmetry would then merge into the ν_4 mode of D_{3h} symmetry, which is expected to occur at about 720 cm^{-1}.[57,58]

3.4. Nano-ESI-TOF-MS. It is known that the choice of diluent influences the stoichiometry of the detected species.[35] Therefore, the nano-ESI-MS spectra were obtained directly with octanolic solutions of $Eu(NO_3)_3 \cdot 6H_2O$ with different concentrations of the C5-BTBP ligand without dilution in standard ESI solvents such as MeOH. Figure 10 shows the MS

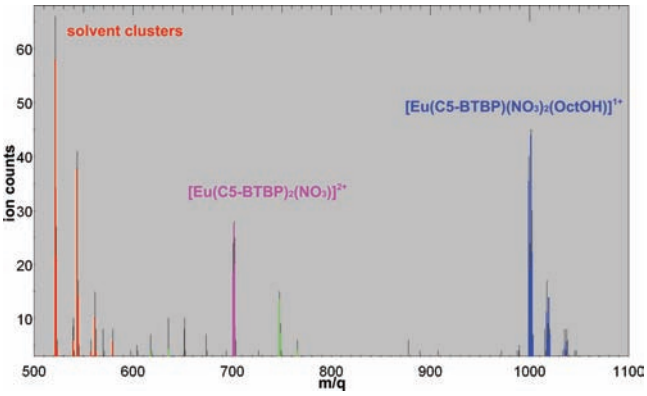

Figure 10. Nano-ESI-MS spectra of 5×10^{-5} mol/L $Eu(NO_3)_3$ in a 1-octanol solution with 2.5×10^{-5} mol/L C5-BTBP. Calculated fits: green, free C5-BTBP; magenta, $[Eu(C5\text{-}BTBP)_2(NO_3)]^{2+}$; dark blue, $[Eu(NO_3)_2(C5\text{-}BTBP)(C_8H_{17}OH)]^+$.

spectrum of a solution of [Eu] = 5×10^{-5} mol/L and [C5-BTBP] = 2.5×10^{-5} mol/L in 1-octanol, where the measured data are plotted in black while the fits of the referring species are plotted in different colors. The species appear as peak clusters because of the solvation shell remaining around the molecules. $[Eu(NO_3)_2(C5\text{-}BTBP)(C_8H_{17}OH)]^+$ is the dominating complex (m/q = 999.4 u/e, 74.3%, blue), while $[Eu(NO_3)(C5\text{-}BTBP)_2]^{2+}$ plays a subordinate role (m/q = 700.9 u/e, 25.7%, magenta). Nevertheless, even at substoichiometric concentrations of C5-BTBP, this 1:2 complex can be detected. The peaks at lower m/q values (red fits) originate from $[C5\text{-}BTBP(H)]^+$.

There is a qualitative difference between $[Eu(NO_3)(C5\text{-}BTBP)_2]^{2+}$ and all other species. It is the only complex not attaching water molecules, suggesting that it is more hydrophobic than the other complexes. Neither the metal center nor the nitrate anion seems to be able to attach water in this complex. Increasing the C5-BTBP concentration to 1×10^{-4} mol/L (Figure 11) leads to an increase of the relative

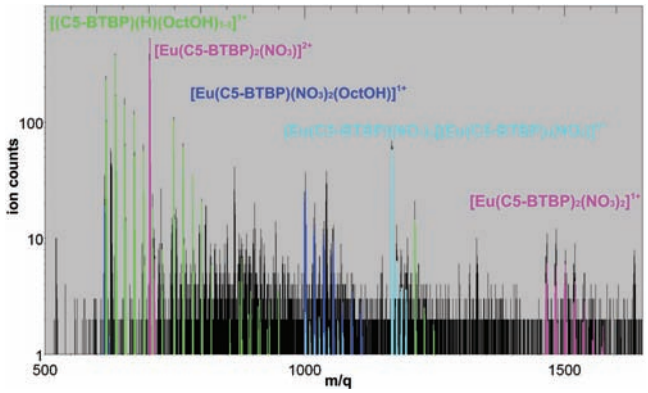

Figure 11. Nano-ESI-MS spectra of 5×10^{-5} mol/L $Eu(NO_3)_3$ in a 1-octanol solution with 1×10^{-4} mol/L C5-BTBP. Calculated fits: green, free C5-BTBP; magenta, $[Eu(C5\text{-}BTBP)_2(NO_3)]^{2+}$ and $[Eu(NO_3)_2(C5\text{-}BTBP)_2]^+$; dark blue, $[Eu(NO_3)_2(C5\text{-}BTBP)\text{-}(C_8H_{17}OH)]^+$; cyan, $[Eu(NO_3)_3(C5\text{-}BTBP)][Eu(NO_3)(C5\text{-}BTBP)_2]^{2+}$. Note that the MS spectrum is plotted on a logarithmic scale to visualize minor species and isotopic patterns.

abundance of the 1:2 complexes ($[Eu(NO_3)(C5\text{-}BTBP)_2]^{2+}$ m/q = 700.9 u/e, 59.9%, magenta), while the abundance of the 1:1 complex decreases ($[Eu(NO_3)_2(C5\text{-}BTBP)(C_8H_{17}OH)]^+$ m/q = 999.4 u/e, 8%, blue). Besides the Eu-C5-BTBP species in the first spectrum, two other complexes emerge at higher ligand concentration: the $[Eu(NO_3)_2(C5\text{-}BTBP)_2]^+$ complex (m/q = 1463.6 u/e, 3.3%, magenta) and a dimeric complex $[Eu(NO_3)_3(C5\text{-}BTBP)][Eu(NO_3)(C5\text{-}BTBP)_2]^{2+}$ (m/q = 1166.5 u/e, 28.8%, cyan). In contrast to the $[Eu(NO_3)(C5\text{-}BTBP)_2]^{2+}$ complex, the $[Eu(NO_3)_2(C5\text{-}BTBP)_2]^+$ complex attaches some water molecules. Hence, the hydrophobic character of the latter complex seems to be lower, which corroborates the hypothesis of inner-sphere coordination of one nitrate ion in this case.

The nano-ESI-TOF-MS spectrometry data confirm that, at high ligand concentrations (which are used in extraction experiments), the formation of the 1:2 complexes is favored; $[Eu(BTBP)_2(NO_3)]^{2+}$ and $[Eu(BTBP)_2(NO_3)_2]^+$ are the dominating complexes. In similar experiments, Retegan et al. drew the conclusion that one nitrate is coordinated to the metal center in the 1:2 complexes.[12] The presented spectra in an octanolic solution in the present work also point to coordination of one nitrate ion in the first shell. In contrast to all other detected species, the $[Eu(BTBP)_2(NO_3)]^{2+}$ complexes do not seem to attach water molecules during the ESI process. Hence, these species seem to be very hydrophobic, being evidence for a shielding of the nitrate ion by the hydrophobic moieties of the BTBP ligands. In contrast, the $[Eu(BTBP)_2(NO_3)_2]^+$ complexes, being present in solution at higher ligand concentrations, remain in a small solvent shell.

dx.doi.org/10.1021/ic202119x | *Inorg. Chem.* 2012, 51, 591–600

This suggests that the second nitrate ion is located in a second sphere, allowing the attachment of water molecules.

4. CONCLUSIONS

The investigation of the complexation of Eu^{III} by different BTBP ligands in an octanolic solution with complementary methods revealed a diverse behavior of the investigated BTBP ligands. Depending on the bulkiness of the respective moieties the probability to find an anion or a quenching solvent molecule coordinated to the metal center varies. Thus, using the weakly coordinating perchlorate anion, the fluorescence lifetime increased with increasing steric demand of the BTBP ligand. In contrast, in the solid state, even weakly coordinating anions may coordinate to the metal center in 1:2 complexes of sterically demanding ligands such as $CyMe_4$-BTBP. Care should therefore be taken when comparing complexes in solution and in solids. Steric effects are also important for Eu-BTBP 1:2 complexes in solution with nitrate as the counterion. VSB spectroscopic investigations showed clearly that the coordination of a nitrate anion can occur when the alkyl chains of the BTBP ligands are relatively short. In addition, MS results show that $[Eu(C5\text{-}BTBP)_2(NO_3)]^{2+}$ has a more hydrophobic character compared to the other detected complex species.

■ ASSOCIATED CONTENT

Supporting Information

Titrations of Eu^{III} with BTBP ligands monitored with $^5D_0 \rightarrow {}^7F_0$ emission spectra (Figure S1) and crystallographic data in CIF format of **1** and **2**. This material is available free of charge via the Internet at http://pubs.acs.org.

■ AUTHOR INFORMATION

Corresponding Author

*E-mail: michael.steppert@kit.edu.

■ ACKNOWLEDGMENTS

Financial support for this research was provided by the European Commission (Project ACSEPT, Contract No. FP7-CP-2007-211 267). M.S. acknowledges financial support by the Helmholtz–Russia Joint Research Group HRJRG011.

■ REFERENCES

(1) OECD. *Actinide and fission product partitioning and transmutation, status and assessment report*; OECD Nuclear Energy Agency: Paris, 1999.

(2) Lewis, F. W.; Harwood, L. M.; Hudson, M. J.; Drew, M. G. B.; Desreux, J. F.; Vidick, G.; Bouslimani, N.; Modolo, G.; Wilden, A.; Sypula, M.; Vu, T. H.; Simonin, J. P. *J. Am. Chem. Soc.* **2011**, *133* (33), 13093–13102.

(3) Benay, G.; Schurhammer, R.; Wipff, G. *Phys. Chem. Chem. Phys.* **2011**, *13* (7), 2922–2934.

(4) Foreman, M. R. S. J.; Hudson, M. J.; Geist, A.; Madic, C.; Weigl, M. *Solvent Extr. Ion Exch.* **2005**, *23* (5), 645–662.

(5) Nilsson, M.; Andersson, S.; Drouet, F.; Ekberg, C.; Foreman, M. R. S. J.; Hudson, M. J.; Liljenzin, J. O.; Magnusson, D.; Skarnemark, G. *Solvent Extr. Ion Exch.* **2006**, *24* (3), 299–318.

(6) Nilsson, M.; Ekberg, C.; Foreman, M. R. S. J.; Hudson, M. J.; Liljenzin, J. O.; Modolo, G.; Skarnemark, G. *Solvent Extr. Ion Exch.* **2006**, *24* (6), 823–843.

(7) Fermvik, A.; Ekberg, C.; Englund, S.; Foreman, M. R. S. J.; Modolo, G.; Retegan, T.; Skarnemark, G. *Radiochim. Acta* **2009**, *97* (6), 319–324.

(8) Retegan, T.; Ekberg, C.; Dubois, I.; Fermvik, A.; Skarnemark, G.; Wass, T. J. *Solvent Extr. Ion Exch.* **2007**, *25* (4), 417–431.

(9) Ekberg, C.; Aneheim, E.; Fermvik, A.; Foreman, M.; Löfström-Engdahl, E.; Retegan, T.; Spendlikova, I. *J. Chem. Eng. Data* **2010**, *55* (11), 5133–5137.

(10) Hubscher-Bruder, V.; Haddaoui, J.; Bouhroum, S.; Arnaud-Neu, F. *Inorg. Chem.* **2010**, *49* (4), 1363–1371.

(11) Aneheim, E.; Ekberg, C.; Fermvik, A.; Foreman, M. R. S. J.; Retegan, T.; Skarnemark, G. *Solvent Extr. Ion Exch.* **2010**, *28* (4), 437–458.

(12) Retegan, T.; Berthon, L.; Ekberg, C.; Fermvik, A.; Skarnemark, G.; Zorz, N. *Solvent Extr. Ion Exch.* **2009**, *27* (5), 663–682.

(13) Magnusson, D.; Christiansen, B.; Foreman, M. R. S.; Geist, A.; Glatz, J. P.; Malmbeck, R.; Modolo, G.; Serrano-Purroy, D.; Sorel, C. *Solvent Extr. Ion Exch.* **2009**, *27* (2), 97–106.

(14) Magnusson, D.; Christiansen, B.; Malmbeck, R.; Glatz, J. P. *Radiochim. Acta* **2009**, *97* (9), 497–502.

(15) Geist, A.; Hill, C.; Modolo, G.; Foreman, M. R. S. J.; Weigl, M.; Gompper, K.; Hudson, M. J.; Madic, C. *Solvent Extr. Ion Exch.* **2006**, *24* (4), 463–483.

(16) Foreman, J.; Hudson, M. J.; Drew, M. G. B.; Hill, C.; Madic, C. *Dalton Trans.* **2006**, No. 13, 1645–1653.

(17) Hudson, M. J.; Boucher, C. E.; Braekers, D.; Desreux, J. F.; Drew, M. G. B.; Foreman, M. R. S. J.; Harwood, L. M.; Hill, C.; Madic, C.; Marken, F.; Youngs, T. G. A. *New J. Chem.* **2006**, *30* (8), 1171–1183.

(18) Trumm, S.; Lieser, G.; Foreman, M. R. S. J.; Panak, P. J.; Geist, A.; Fanghänel, T. *Dalton Trans.* **2010**, *39* (3), 923–929.

(19) Vu, T. H. *Étude par spectrométrie de fluorescence de la solvatation et de la complexation des ions Eu(III) en milieu octanol et à l'interface avec l'eau*; CEA-R-6229; Commissariat à l'énergie atomique: Saclay, France, 2009.

(20) Schmidt, M.; Stumpf, T.; Fernandes, M. M.; Walther, C.; Fanghänel, T. *Angew. Chem., Int. Ed.* **2008**, *47* (31), 5846–5850.

(21) Stumpf, T.; Fanghänel, T.; Grenthe, I. *J. Chem. Soc., Dalton Trans.* **2002**, No. 20, 3799–3804.

(22) Stumpf, S.; Stumpf, T.; Walther, C.; Bosbach, D.; Fanghänel, T. *Radiochim. Acta* **2006**, *94*, 243–248.

(23) Stumpf, T.; Tits, J.; Walther, C.; Fanghänel, T. *J. Colloid Interface Sci.* **2004**, *276* (1), 118–124.

(24) Colette, S.; Amekraz, B.; Madic, C.; Berthon, L.; Cote, G.; Moulin, C. *Inorg. Chem.* **2004**, *43* (21), 6745–6751.

(25) Denecke, M. A.; Rossberg, A.; Panak, P. J.; Weigl, M.; Schimmelpfennig, B.; Geist, A. *Inorg. Chem.* **2005**, *44* (23), 8418–8425.

(26) Denecke, M. A.; Panak, P. J.; Burdet, F.; Weigl, M.; Geist, A.; Klenze, R.; Mazzanti, M.; Gompper, K. *C. R. Chem.* **2007**, *10* (10–11), 872–882.

(27) Trumm, S.; Panak, P. J.; Geist, A.; Fanghänel, T. *Eur. J. Inorg. Chem.* **2010**, *19* (19), 3022–3028.

(28) Dole, M.; Mack, L. L.; Hines, R. L.; Mobley, R. C.; Ferguson, L. D.; Alice, M. A. *J. Chem. Phys.* **1968**, *49*, 2240–2249.

(29) Dole, R. B. *Electrospray Ionization Mass Spectrometry—Fundamentals, Instrumentation and Applications*, 1st ed.; John Wiley & Sons: Chichester, U.K., 1997.

(30) Schalley, C. A. *Modern Mass Spectrometry*; Springer: New York, 2003.

(31) Pramanik, B. N.; Ganguly, A. K.; Gross, M. L. *Applied Electrospray Mass Spectrometry*; Marcel Dekker: New York, 2002.

(32) Walther, C.; Rothe, J.; Fuss, M.; Büchner, S.; Koltsov, S.; Bergmann, T. *Anal. Bioanal. Chem.* **2007**, *388* (2), 409–431.

(33) Walther, C.; Fuss, M.; Büchner, S. *Radiochim. Acta* **2008**, *96*, 411–425.

(34) Walther, C.; Rothe, J.; Brendebach, B.; Fuss, M.; Altmaier, M.; Marquardt, C. M.; Büchner, S.; Cho, H. R.; Yun, J. I. *Radiochim. Acta* **2009**, *97*, 199–207.

(35) Steppert, M.; Walther, C.; Geist, A.; Fanghänel, T. *New J. Chem.* **2009**, *33* (12), 2437–2442.

(36) Colette, S.; Amekraz, B.; Madic, C.; Berthon, L.; Cote, G.; Moulin, C. *Inorg. Chem.* **2002**, *41* (26), 7031–7041.

(37) Colette, S.; Amekraz, B.; Madic, C.; Berthon, L.; Cote, G.; Moulin, C. *Inorg. Chem.* **2003**, *42* (7), 2215−2226.
(38) *SIR2002*; SIR Pty. Ltd.: Terrey Hills, Australia, 2002.
(39) Sheldrick, G. M. *SHELXL97*; University of Göttingen: Göttingen, Germany, 1997.
(40) Choppin, G. R.; Wang, Z. M. *Inorg. Chem.* **1997**, *36* (2), 249−252.
(41) Choppin, G. R.; Peterman, D. R. *Coord. Chem. Rev.* **1998**, *174* (1), 283−299.
(42) Frey, S. T.; Horrocks, W. D. *Inorg. Chim. Acta* **1995**, *229* (1−2), 383−390.
(43) Henrie, D. E.; Fellows, R. L.; Choppin, G. R. *Coord. Chem. Rev.* **1976**, *18* (2), 199−224.
(44) Horrocks, W. D.; Sudnick, D. R. *J. Ant. Chem. Soc.* **1979**, *101*, 334−340.
(45) Kimura, T.; Nagaishi, R.; Kato, Y.; Yoshida, Z. *Radiochim. Acta* **2001**, *89* (3), 125−130.
(46) Tanaka, F.; Kawasaki, Y.; Yamashita, S. *J. Chem. Soc., Faraday Trans. 1* **1988**, *84*, 1083−1088.
(47) Lindqvist-Reis, P.; Walther, C.; Klenze, R.; Eichhöfer, A.; Fanghänel, T. *J. Chem. Phys.* **2005**, *110*, 5279−5285.
(48) Tsaryuk, V.; Savchenko, V. D.; Zolin, V.; Kudryashova, V. A. *Spectrochim. Acta, Part A* **2000**, *56* (6), 1149−1155.
(49) Tsaryuk, V.; Savchenko, V. D.; Aryutkina, N. L.; Chenskaya, T. B. *J. Appl. Spectrosc.* **1994**, *60* (3), 185−192.
(50) Tsaryuk, V.; Zolin, V.; Legendziewicz, J.; Szostak, R.; Gawryszewska, P. *Proc. 4th Int. Spring Workshop Spectrosc., Struct. Synth. Rare Earth Syst.* **2004**, *380* (1−2), 418−425.
(51) Bergmann, T.; Martin, T. P.; Schaber, H. *Rev. Sci. Instrum.* **1989**, *60* (4), 792−793.
(52) Bergmann, T.; Martin, T. P.; Schaber, H. *Rev. Sci. Instrum.* **1989**, *60* (3), 347−349.
(53) Bergmann, T.; Goehlich, H.; Martin, T. P.; Schaber, H.; Malegiannakis, G. *Rev. Sci. Instrum.* **1990**, *61* (10), 2585−2591.
(54) Bergmann, T.; Martin, T. P.; Schaber, H. *Rev. Sci. Instrum.* **1990**, *61* (10), 2592−2600.
(55) Bünzli, J. C. G.; Klein, B.; Chapuis, G.; Schenk, K. J. *J. Inorg. Nucl. Chem.* **1980**, *42* (9), 1307−1311.
(56) Schimmelpfennig, B. Personal communication, 2010.
(57) Volkov, S. V.; Evtushenko, N. P.; Yatsimirskii, K. B. *Teor. Éksp. Khim.* **1973**, *9* (2), 273−278.
(58) Perelygin, I. S.; Mikhailov, G. P. *Zh. Prikl. Spektrosk.* **1988**, *48* (5), 766−772.